Chain formation of spheres in oscillatory fluid flows

D. Klotsa, Michael R. Swift, R. M. Bowley, and P. J. King
School of Physics and Astronomy, University of Nottingham, Nottingham, NG7 2RD, United Kingdom
(Received 28 October 2008; published 9 February 2009)

A collection of spherical particles subjected to horizontal oscillatory fluid flow is known to form chains perpendicular to the direction of the oscillation. We have developed computer simulations to model such a system and have validated them against experiments carried out in a small fluid-filled cell. In both experiment and simulation we find that the particles go through the same stages of evolution from a dispersed initial configuration to an ordered chain structure. We then use our computer simulations to investigate in detail the interactions responsible for chain formation and the interaction between fully formed chains.

DOI: 10.1103/PhysRevE.79.021302 PACS number(s): 45.70.Qj, 47.55.Kf, 05.65.+b

I. INTRODUCTION

In the last few years, there has been a lot of interest in pattern formation involving granular materials [1]. For example, dry granular beds under vibration have been found to form surface patterns [2] or stripes [3]. Grains, which are fully immersed in a fluid, exhibit a richer pattern-forming behavior due to the interaction between the particles and the fluid [4–7]. Related ordering phenomena have recently been observed for bubbles in an oscillated fluid [8].

Wunenburger *et al.* [9] performed experiments in which a water-filled cell containing bronze particles was subjected to horizontal sinusoidal vibration. They observed the formation of periodic chains of particles, aligned perpendicular to the direction of oscillation, and suggested that the interaction between particles seems to arise from the steady streaming flow [10] induced by the vibration. In another experiment, Voth *et al.* [11] found that spherical particles formed regular lattices under vertical vibration in a viscous fluid. They showed that a model based on steady streaming can be used to explain the attractive part of the interaction leading to the formation of the pattern.

In order to investigate the interaction further, Klotsa *et al.* [12] studied a simpler system consisting of two spheres in a fluid-filled cell under horizontal vibration. The pair was found to align perpendicular to the direction of oscillation with the two spheres separated by a well-defined distance. It was confirmed that the interaction between the two spheres is related to the steady streaming flow.

In the present study we build on our earlier work by considering the interactions between many particles in a fluid subjected to horizontal vibration. We investigate how these interactions give rise to the formation of chains of spheres using both experiments and simulations. The outline of the paper is as follows. In Sec. II we describe the experimental arrangement and in Sec. III we explain the simulation method that we have used to model our experiments. In order to understand the mechanism leading to chain formation we need to study steady streaming flows in a confined geometry, a topic which is introduced in Sec. IV. Section V describes the formation and evolution of chains, comparing experiments and simulations. Details of the chain-forming mechanism from simulation are given in Sec. VI. We end with a brief discussion of pattern formation in Sec. VII.

II. EXPERIMENTAL ARRANGEMENT

We conduct our experiments using spheres fully immersed in a liquid contained in a small cell which is subjected to horizontal vibration. Specifically, the cell was constructed in the following way. A rectangular hole was cut into a 3-mm-thick rubber sheet which was sandwiched between two glass plates, supported by an aluminum alloy frame. The dimensions of the resulting liquid-tight region were 39.5 mm long (x direction, horizontal), 11.5 mm wide (y direction, horizontal), and 3 mm deep (z direction, vertical). The liquid and the spheres were placed in the cell before it was sealed. The cell was mounted between two long-throw loudspeakers so that the plane of the glass sheets (x-y plane) was accurately horizontal during vibratory motion such that only one-dimensional motion in the x direction occurred. The sinusoidal motion may be characterized by the frequency f and by the dimensionless acceleration of the cell, $\Gamma = A\omega^2/g$, which was determined using capacitative acceleration sensors. Here A is the amplitude of the vibration, $\omega = 2\pi f$ is the angular frequency, and g is the gravitational acceleration.

We used a solution of glycerol and water with kinematic viscosity $\nu = 2.0 \times 10^{-6}$ m^2 s^{-1} at 22 °C. The laboratory and cell were kept at this temperature to avoid changes in the viscosity. The fluid density was 1060 kg m^{-3}. The fluid was pumped prior to the experiment so as to remove any dissolved air. The cell was then sealed so that no air was trapped in it. The particles used were nonmagnetic, stainless-steel spheres, 1 mm in diameter and of density 7950 kg m^{-3}. A high-speed camera (up to 1000 frames/s) was mounted directly above the cell so that the motion of the spheres could be displayed on a monitor and recorded.

Because the liquid is nearly incompressible it moves with the cell. The spheres, being more dense than the fluid, initially rest on the base of the cell. Under vibration the spheres will be influenced by fluid drag forces and by the frictional interaction with the base. Since the steel spheres and the liquid have different densities, there is a relative amplitude of motion of the spheres with respect to the liquid, A_r, which is smaller than the driving amplitude A. All the experiments reported here were carried out at $f = 50$ Hz and with $\Gamma = 6.5$. The corresponding relative amplitude A_r was measured to be 0.5 ± 0.05 mm, whereas the driving amplitude was $A = 0.65$ mm. We observed that, under vibration, there is hardly

any rotation of the spheres, implying that they slip on the lower glass surface for most of the oscillation cycle [9,12].

III. SIMULATION METHOD

The fluid and the spheres were modeled using a simplified version of the method developed by Kalthoff *et al.* [13]. The fluid was assumed to be incompressible and described by the three-dimensional Navier-Stokes' equation and the continuity equation

$$\frac{\partial \mathbf{v}}{\partial t} + (\mathbf{v} \cdot \nabla)\mathbf{v} = -\frac{1}{\rho}\nabla P + \nu \nabla^2 \mathbf{v} - \mathbf{g}, \tag{1}$$

$$\nabla \cdot \mathbf{v} = 0. \tag{2}$$

Here $\mathbf{v}$ is the fluid velocity, P is the fluid pressure, ρ is the fluid density, and $\mathbf{g}$ is the acceleration due to gravity, along the vertical axis (z). These equations are discretized on a staggered marker-and-cell mesh [14] and solved using the projection method [15]. The incompressibility constraint is satisfied via an explicit operator-splitting technique, described in detail in Ref. [16]. This results in Poisson's equation for the pressure, which is readily solved numerically using Fourier techniques.

The spheres were treated as objects fully immersed in the fluid. The fluid-solid coupling was introduced by enforcing the no-slip boundary condition on the surface of the spheres. This was achieved numerically by assuming that the fluid permeates the spheres and that the fluid inside each sphere moves with the instantaneous velocity of the sphere. At each time step, the spheres' velocities were transferred to the fluid at the sites occupied by the spheres. The fluid subsequently evolved according to the Navier-Stokes' equation, ensuring that the continuity equation was satisfied. The force on each sphere, $\mathbf{F}_s$, was then calculated from

$$\mathbf{F}_s = \sum_i (-\nabla P + \nu \rho \nabla^2 \mathbf{v}), \tag{3}$$

where the sum was taken over all sites occupied by the sphere. The derivatives in Eq. (3). were calculated using finite-difference approximations. This force was then used to update the sphere's position using molecular dynamics techniques [17]. Collisions between particles, when present, were modeled using soft-sphere molecular dynamics [18].

Under vibration the spheres slide on the lower surface of the cell. To avoid the complications associated with lubrication forces, the spheres were prevented from reaching the lowest cells of the fluid grid by a contact force which constrained them to be at least one lattice spacing above the true cell boundary. Nor did we include the frictional interaction between the spheres and the surface, which is known to be complex [9]. However, the ratio of frictional forces to the oscillatory drag forces is estimated to be quite small, of order 0.1 or less [19].

The simulations were carried out using a time step $\Delta t = 10^{-6}$ s and a grid spacing $\Delta x = 7.5 \times 10^{-5}$ m. In some of the simulations, we used a rectangular slab with dimensions $39.5 \times 11.5 \times 3$ mm^3, as in experiments. In the rest we used a square box with dimensions $30 \times 30 \times 3$ mm^3 so as to study interactions between particles or chains which are far from walls.

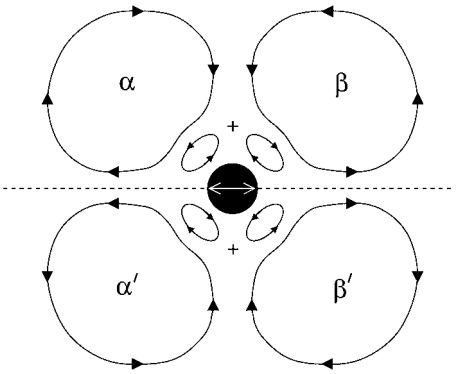

FIG. 1. Schematic diagram showing the streaming flow for a single oscillating sphere, in the plane through the sphere. The double-arrowed line on the sphere indicates the direction of oscillation. There is rotational symmetry about the axis of oscillation (x), indicated by the dashed line. There are four vortex rings: two on the left and two on the right of the sphere. The crosses indicate stagnation points and α, α' and β, β' label the two outer vortex rings.

Two types of simulation have been performed. In one, the system was chosen to model the experimental arrangement as closely as possible. The box and the fluid were oscillated and the spheres were free to respond to the oscillation. The driving amplitude $A = g\Gamma/\omega^2$ was tuned so that the relative amplitude of the spheres with respect to the fluid was the same as in the experiment, $A_r = 0.5$ mm. In the other type of simulation, the spheres were fixed at some constant relative position and were both oscillated sinusoidally with relative amplitude $A_r = 0.5$ mm with respect to the fluid. Here, the fluid flow was generated by the motion of the spheres. Once a steady state had been reached (that is, the fluid velocities oscillated periodically at the driving frequency) the time-averaged forces on the spheres and the corresponding fluid flows could be determined.

IV. STEADY STREAMING

The concept of steady streaming around a single isolated oscillating sphere in an infinite fluid has been studied analytically and numerically [20–25]. The parameters that govern such a system are the viscosity ν, frequency f, sphere diameter d, and relative amplitude A_r. Consequently there are three independent length scales, A_r, d, and the viscous penetration depth $\delta = \sqrt{\nu/\omega}$. In our experiments and simulations, $A_r = 0.5$ mm, $d = 1$ mm, and $\delta = 0.08$ mm. There have been a variety of studies of steady streaming over different regions in this parameter space, as summarized in [21].

Figure 1 shows a schematic diagram of the time-averaged fluid flow around a single, oscillating sphere in an infinite liquid. The diagram shows the flows in a plane through the center of the sphere. The sphere oscillates along the x axis in this plane, as shown by the dashed line. The solid lines are representative streamlines for the steady streaming flow. In this plane there are eight vortices, four inner (primary

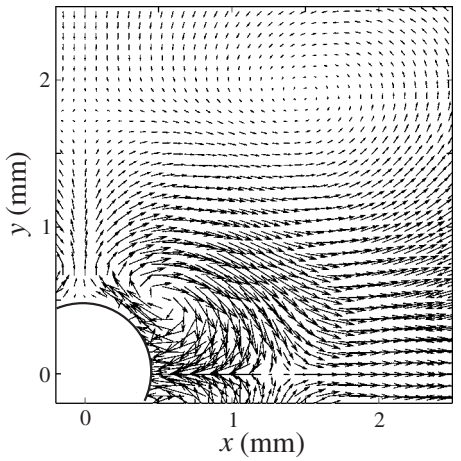

FIG. 2. Vector plot taken from simulations, showing part of the time-averaged fluid flow around a single oscillating sphere. The sphere is oscillating in the x direction and the fluid flow in the x-y plane passing through the center of the sphere is shown. The arrows indicate the local direction of the streaming flow. For reasons of clarity, the magnitude of the arrows is proportional to the product of the local speed and the square of the distance from the origin.

streaming) and four outer (secondary streaming). In three dimensions there is rotational symmetry about the x axis and the eight vortices shown in Fig. 1 are cross sections through four circular vortex rings, two inner and two outer. For example, α-α' are cross sections through the same single outer vortex ring. The sense of circulation of each vortex ring can be inferred from the direction of the arrowheads on each streamline. Note that the outer vortex rings have opposite circulation to their nearer inner vortex ring.

In our system, however, the particles are moving in a finite box, along the bottom surface. We have carried out simulations in order to determine the influence of the confining geometry on the streaming flows. In Fig. 2 we show data from simulations for a single oscillating sphere. The vector plot of Fig. 2 is the time-averaged fluid flow over one cycle of oscillation after a steady state has been reached, typically after about 0.5 s. The vector plot shown is a slice taken in the horizontal x-y plane at a height through the sphere's center. Only one quadrant is shown. The flow is similar in form to the corresponding quadrant in Fig. 1.

The presence of the bottom surface breaks the full rotational symmetry of the flow about the x axis. What remains is approximately half of the flow generated by a single, isolated sphere. Figure 3 shows a vector plot through the center of the sphere in the x-z plane. It can be seen that the streaming flow is similar to the flow that would have been generated in the half space $z>0$, were the bottom surface not present. The vortex rings (inner and outer) terminate on the lower surface of the cell, forming open-ended vortex loops. A similar change in the fluid flow due to the presence of a surface has recently been observed experimentally [21]. Figure 4 is a schematic diagram of the flows shown in Fig. 3, included here for clarity. Note that the flow is somewhat squashed in the z direction due to the top surface of the cell.

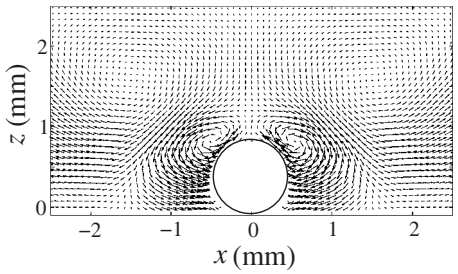

FIG. 3. Vector plot taken from simulations, showing part of the time-averaged fluid flow around a single oscillating sphere. The sphere is oscillating in the x direction and the fluid flow in the x-z plane passing through the centre of the sphere is shown. The rotational symmetry about the x axis is broken by the bottom surface. The vortex rings have now become open-ended vortex loops terminating on the base of the cell. For reasons of clarity, the magnitude of the arrows is proportional to the product of the local speed and the square of the distance from the mean position of the center of the sphere.

V. EVOLUTION OF CHAINS

First we describe the experiments. Sixty-four spheres were initially placed in the cell which was then mounted onto the vibratory apparatus and manipulated so that the particles were widely dispersed. The cell was then vibrated at $f=50$ Hz and $\Gamma=6.5$, giving $A_r=0.5$ mm. The subsequent motion of the spheres was recorded on the high-speed camera and replayed at a low frame-per-second rate so that the process could be observed in detail.

In Fig. 5 we show a few snapshots which are characteristic of the evolution of the pattern together with their corresponding times. As soon as the vibration is switched on, nearby particles align in pairs, the line joining their centers tending to orient perpendicular to the direction of the oscillation. A free particle moves so that it joins the nearest pair to form a short chain. Similarly, a free pair joins another nearby pair also forming a short chain. There is a tendency for particles and chains to attach to the long sides of the cell. Short chains then evolve to form longer ones by attaching at the ends of the nearest chain. Long chains form which span the cell between the two long sides. The stages described so far have occurred within the first 2 s of oscillation. Everything that follows happens at a much slower rate as the system evolves toward its final configuration (by about 10 s) in which there are no free particles or free chains.

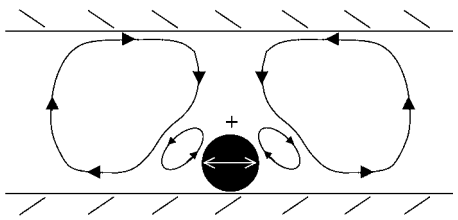

FIG. 4. Schematic diagram showing the streaming flow in the x-z plane through the center of the sphere. The double-arrowed line on the sphere indicates the direction of oscillation. This diagram should be compared to Fig. 3.

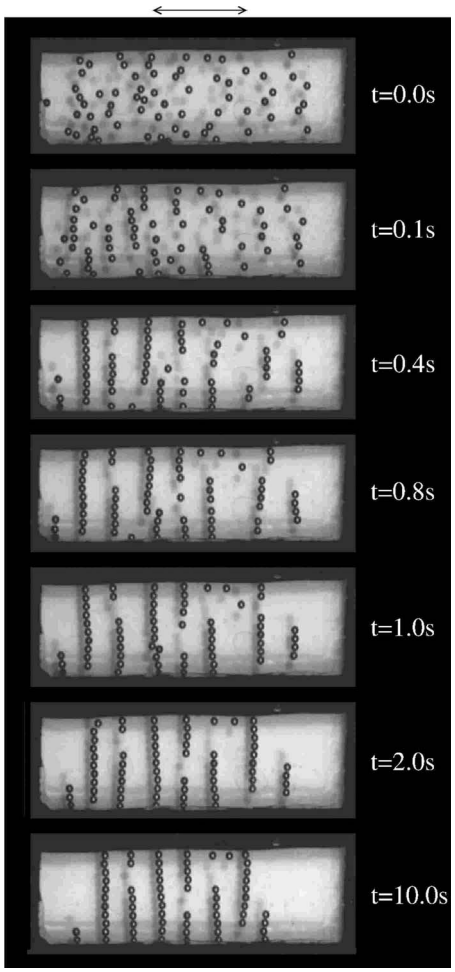

FIG. 5. Series of snapshots, taken from experiment, showing the evolution of 64 spheres from an initial dispersed configuration at $t=0$, to an ordered state after 10.0 s, under horizontal vibration. By 0.1 s, the nearest spheres have interacted with each other; pairs have started to form, aligning perpendicular to the direction of oscillation. Between 0.1 and 0.4 s, short chains form; there is also a tendency for particles and chains to attach to the side walls. Between 0.4 and 1.0 s, short chains evolve to form longer ones by attaching at the ends of the nearest chain; or they attach to the sidewalls; any free particles move toward the sidewalls or attach at the ends of the nearest chain. After 2.0 s, most particles are either part of a chain or attached to the wall; there are no free particles. Thereafter the arrangement appears to be more or less stable.

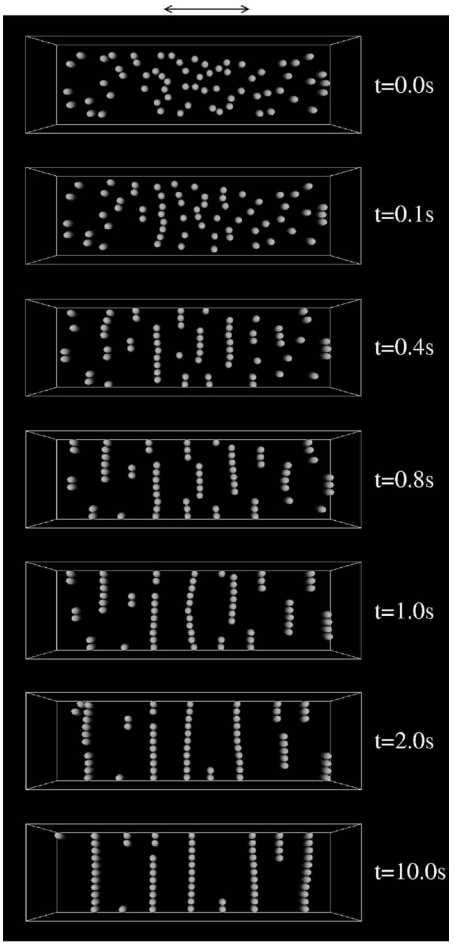

FIG. 6. Series of snapshots taken from a simulation of the experimental system shown in Fig. 5. The particles go through the same stages of evolution, even though the initial positions and the final stable configuration differ. The time scales for the evolution are also comparable.

The experiment has been repeated several times under the same vibratory conditions but with different initial positions of the spheres. Each time the exact positions of the spheres in the final configuration are different. However, the time scale for the evolution is always the same, and the system goes through the same stages of evolution, outlined in the previous paragraph and shown in Fig. 5, always resulting in a more or less stable chain configuration.

The particles in Fig. 5 that form a chain appear to be in contact. However, from previous studies [12] it is known that two particles forming a pair have a well-defined gap between them. Under the vibratory conditions considered here, the gap is quite small.

We have carried out simulations using the same parameters and geometry as in the experiment. Even though the initial positions of the particles were different from those in the experiments, similar chain patterns formed over the same time scale, as illustrated in Fig. 6. We observed the same behavior as in the experiments. For example, by 0.4 s pairs could be seen and chains have already started to form, by 2.0 s most chains were attached to the walls, and by 10.0 s the system was more or less stable. Simulations with different initial positions of particles led to different final chain configurations but all went through similar stages of evolution.

Let us define a "full chain" to be one that is aligned perpendicular to the direction of vibration and has the correct number of particles to just span the cell. In both experiments and simulations, we notice that once a full chain has formed, it is stable. However, in some cases chains may merge, giving an excess of particles compared to a full chain, as in Fig. 5 at 1.0 s. The extra particle then acts as a defect which moves up and down the chain. Eventually a particle may leave the chain. The freed particle can then join a neighboring chain, or go to the nearest wall. In other cases two in-

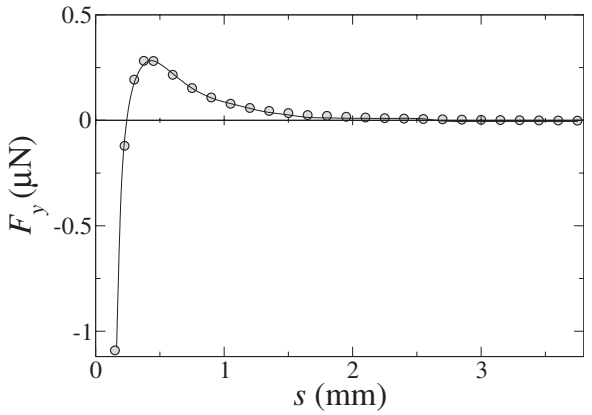

FIG. 7. Interaction force F_y on a single sphere oscillating parallel to a nearby wall. The graph shows F_y plotted as a function of the separation of the nearest surface of the sphere to the wall, s. A positive force indicates an attraction.

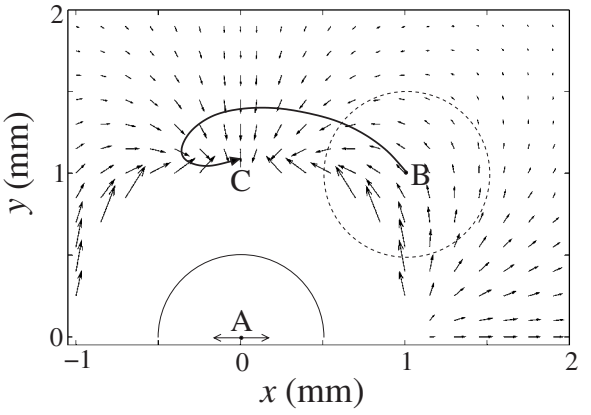

FIG. 8. Vector plot of the effective force acting at the center of particle B placed near particle A. The stable point occurs at C where the force is zero. When particle B is at point C, the gap between the particles is about 0.1 mm. The length of the largest arrow in the figure corresponds to a force of magnitude 2.6 μN. The bold-arrowed line from B to C shows the trajectory followed by B, relative to A, were it free to move. The double arrow at A indicates the direction of oscillation.

complete chains align attached to opposite walls; this looks like a chain with some particles missing. Examples can be seen in Fig. 5 from 2.0 s and in Fig. 6 from 1.0 s. Because the system tries to produce full chains, the free end of an incomplete chain attracts free particles or the free ends of other incomplete chains in its proximity.

The chain configuration is formed in the first few seconds. There may be an occasional random particle that bounces off an end wall or jumps from one chain to another. That apart, the configuration remains stable over the duration of our experiments, typically of the order of minutes.

The similarities between experiment and simulation are evident from Figs. 5 and 6. We are therefore reasonably confident that we can use the same computational model to study the system in more depth. In order to understand the details involved in the formation of chains, we have investigated each step of their development separately, so as to build up a picture which explains the evolution towards a stable configuration. In the following sections we will use simulations to investigate the stages of the evolution: the interaction of a single sphere with a side wall, and the alignment of two spheres; the formation of short chains, and how they interact to produce a long one; the evolution of full chains which span the cell, and the interaction between neighboring full chains.

VI. DETAILS OF CHAIN FORMATION

A. Interaction with the sidewall

A single particle is attracted to a neighboring wall, an effect that is seen in both experiment and simulation. The particle-wall interaction has been studied for a single particle [26–28] and a long-ranged attractive and a short-ranged repulsive force are found for viscous flows [29]. For our system the force acting on a single particle at various distances from a sidewall is shown in Fig. 7. It is attractive at large separations and repulsive at short. The distance at which the force is zero gives the equilibrium separation of the particle from the wall.

B. Two-sphere alignment

When two particles are oscillated in a fluid the pair aligns perpendicular to the direction of oscillation, an effect which has been predicted theoretically for inviscid flows [28], and observed experimentally in viscous flows [9,11,12]. However, the mechanism responsible for the alignment of the pair has not been studied in detail.

In order to estimate the interaction force, we shake two particles A and B in a fluid, while keeping their relative orientation and spacing constant. More specifically, particle A is placed in the center of a square box and one grid point above the bottom surface of the box. Particle B is then placed at some position relative to A in the same plane, as shown in Fig. 8. The fluid is initially at rest. The two spheres are then oscillated with the same amplitude in the x direction, keeping their relative position fixed. The time-averaged force on particle B is measured. The position of particle B is then varied and the process is repeated. In this way we obtain a vector plot showing the force on particle B at various orientations with respect to particle A. Figure 8 shows a vector plot of this force. The length of the arrows gives a measure of the strength of the force.

By studying Fig. 8 we see that there is one stable position for particle B, which is indicated by point C. (We are only showing a portion of the upper half of the space; there is another stable point in the lower half, below particle A.) We remind the reader that in these simulations the particles are locked in position relative to each other, whereas in experiment they are free to move. The bold-arrowed line in Fig. 8 shows the path followed by B, relative to the position of A, in simulations in which the fluid is oscillated and both particles are free to move. This path does not exactly follow the direction of the calculated forces for two reasons: there is a time scale over which the streaming flow is set up, and the moving particles have inertia. Nevertheless, the forces give a reasonable indication of the relative motion of the particles

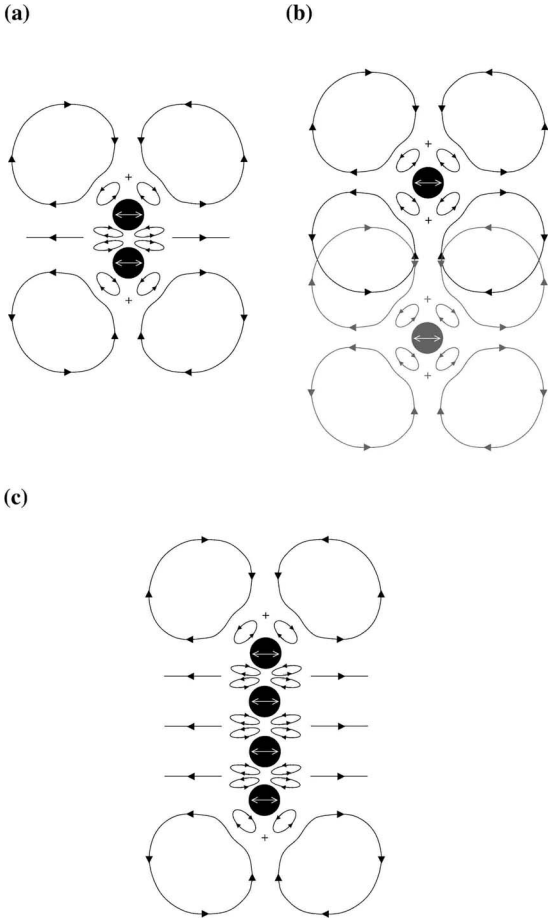

FIG. 9. Schematic diagrams showing the streaming flow in the *x*-*y* plane for a pair of particles and for a four-particle chain. (a) The pair has two outer vortex loops. Here and in subsequent schematic diagrams, the gap between adjacent spheres has been exaggerated to illustrate the inner streaming flow. (b) Two isolated spheres are brought together along a line perpendicular to the direction of oscillation. Initially each particle has two outer vortex loops around it. As the spheres approach each other, the vortex loops of opposite circulation interfere leading to cancellation of the flow. The spheres move toward one another, forming the pair shown in (a). Similarly, when two pairs of spheres approach, they form a short chain, as shown in (c). In each case, the vortex loops are elongated parallel to the chain. Provided these chains do not reach the sidewalls, these vortex loops terminate on the bottom surface of the cell. The double-arrowed line on each sphere indicates the direction of oscillation.

and correctly predict the final configuration of a pair.

It has been proposed in [11] that the interaction between spheres can be understood by considering the streaming flow generated by a single, isolated sphere. If the two spheres are far apart, each particle tends to follow the flow generated by the other. This idea is consistent with our force calculation, shown in Fig. 8. For large separations the forces and the single particle streaming flow, shown in Fig. 2, are in the same direction. However, when the two particles are close together this simple picture breaks down. For example, at the point $x=1$, $y=1$ in Fig. 8, the force points upward and to the left, whereas the flow at the same point in Fig. 2 points downward and to the right.

C. Two-sphere streaming flow

Figure 9(a) shows the streaming flow pattern generated by two spheres in their equilibrium configuration. When the two spheres are brought together, the outer streaming flow resembles that generated by a *single* particle, but with an increased magnitude. The two extra horizontal arrows illustrate the increased flow emerging from the gap between the spheres, in the plane of the spheres [12]. This flow is part of the slightly elongated outer vortex loops, one on either side of the pair. Note that there are only *two* outer vortex loops. It is as if, as the spheres are brought together, the overlapping streaming flows that have opposite circulation partially cancel, lowering the kinetic energy of the system. This is shown schematically in Fig 9(b). Once formed, a pair of spheres is a very stable entity.

D. Formation of a short chain

Our simulations show that the outer streaming flow of a pair of spheres closely resembles that of a single sphere. Therefore, pairs of spheres will interact with other pairs in an analogous fashion to the way single spheres interact, as illustrated in Fig. 8. Consequently, pairs can join together to form short chains. Similarly a pair and a single sphere will interact in the same way.

Figure 9(c) shows the streaming flow for a four-sphere chain in the plane of the spheres. There are only two outer vortex loops, one on either side of the chain. Each vortex loop is elongated in the direction parallel to the chain and terminates on the bottom surface of the cell slightly beyond the ends of the chain. The strength of the outer vortex loops increases with the number of particles in a chain because it is driven by more inner vortex loops. The outer streaming flow pattern has the same structure as that of a single pair. The process of chain interaction continues until the chain becomes full and spans the cell, or there are no more free particles or chains in its vicinity.

As a further elaboration of our picture of chain formation we have run simulations in which two four-particle chains are free to move within an oscillated, fluid-filled cell. A series of snapshots are shown in Fig. 10. Initially, the two small chains are placed almost parallel to each other in the *x*-*y* plane, aligned perpendicular to the direction of oscillation. Each chain remains intact and moves as if it were a single object. The chains "slide" past each other in the *y* direction and move slightly further apart. Eventually the nearest ends of each chain attract each other and join together to form one longer chain. This behavior is consistent with the streaming flow for a short chain shown in Fig. 9(c). The trajectory followed by the chains is similar to that followed by two spheres when forming a pair.

E. Full chains

The addition of particles to a chain continues and short chains get longer. Subsequently the chain is attached to a wall and as more particles attach to the free end, it can form

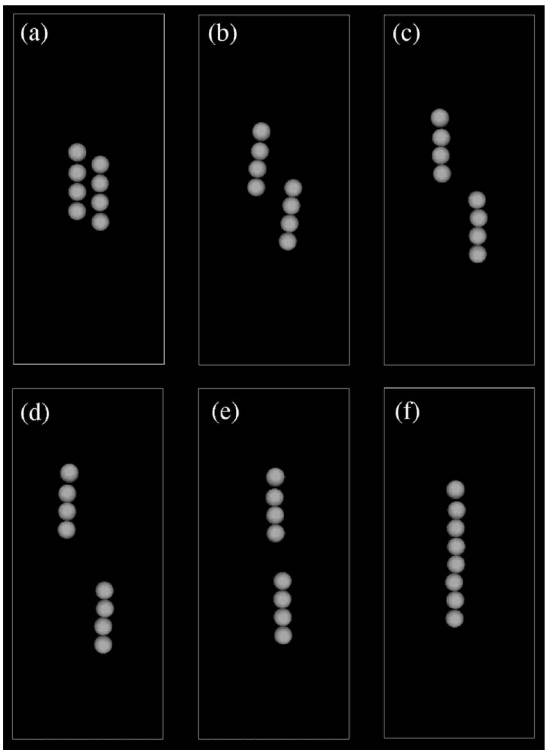

FIG. 10. Sequence of snapshots from a simulation showing the formation of a single chain from two shorter chains. The times are (a) 0, (b) 0.2, (c) 0.3, (d) 0.5, (e) 1.4, and (f) 1.7 s. Each frame shows a small part of the simulated area.

a full chain which spans the width of the cell. In both simulation and experiment these full chains are stable. The streaming flow for a full chain, in a plane through the center of the spheres, is shown in Fig. 11. In this plane the outer streaming flow is directed away from the chain. The return path lies above the spheres; there is no return flow in the plane of the spheres. The ends of the outer vortex loop terminate on the sidewalls instead of on the bottom surface of the cell, forming a vortex line which spans the cell.

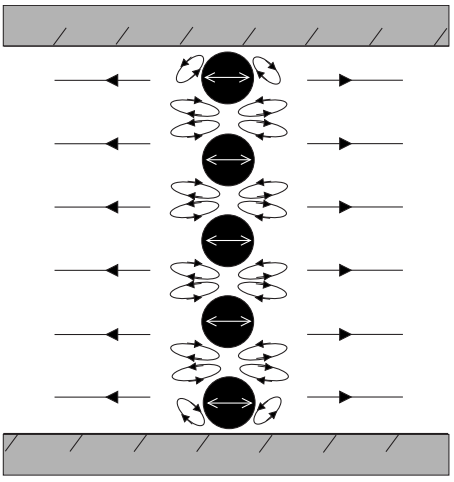

FIG. 11. Schematic diagram showing the streaming flow in an x-y plane through the centers of the spheres for a full chain which spans the cell—we have shown only five spheres for clarity. The vortex loops are parallel to the chain and end at the walls rather than on the bottom surface as they did in Fig. 8(c). The double-arrowed line on each sphere indicates the direction of oscillation.

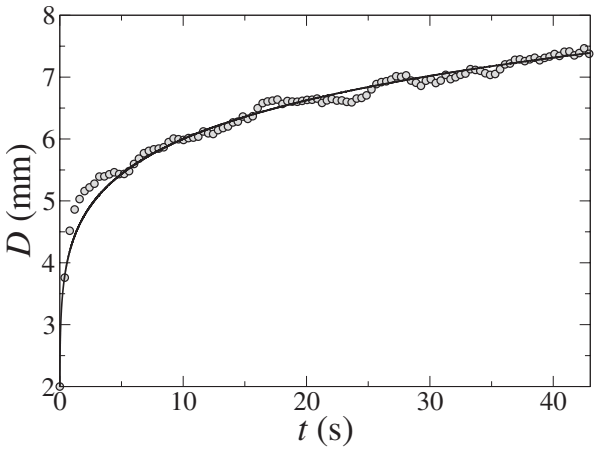

FIG. 12. Mean separation between two full chains as a function of time. The points are from simulations and the line is the theoretical fit discussed in the text.

F. Interactions between full chains

So far we have focused on the interactions between particles that lead to the formation of full chains. From studying Figs. 5 and 6, one might suppose that there is also an interaction between full chains, possibly leading to a well-defined spacing. In order to understand the interaction between full chains we have carried out simulations starting with two full chains separated by 2.0 mm, a separation which is small compared to the steady state separation shown in Fig. 6 at 10.0 s. The cell is oscillated and the particles are free to move in response to the oscillation. We observe that the chains remain intact but drift apart. Their mean separation as a function of time is shown in Fig. 12. The separation between the chains increases with time, which suggests that the interaction between chains is solely repulsive.

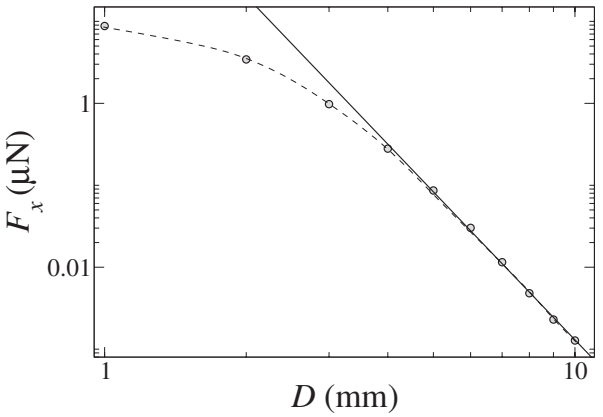

FIG. 13. Time-averaged repulsive force between two full chains as a function of their separation. The solid line shows the asymptotic dependence of the force, as discussed in the text. The dashed line is a guide to the eye.

The repulsive interaction that we observe may be traced to the streaming flow generated by a single full chain, illustrated in Fig. 11. In the plane of the spheres, the flow is always away from the chain; there is no return flow in this plane. It is the flow away from the spheres which tends to push the chains apart.

Further evidence for the existence of a repulsive force due to streaming flows can be obtained by measuring the time-averaged force between chains that are held at a fixed separation. This method is analogous to the force measurement between two single spheres described in Sec. VI B. The mean force on each chain, F_x, is shown in Fig. 13. The force is always repulsive but decreases rapidly with separation D. The solid line is an approximate asymptotic fit showing that $F_x \sim D^{-6}$.

The calculation of the time-averaged force assumes that the relative position of the chains is fixed. If the motion of the chains is sufficiently slow, we can use this force to determine their motion. In this limit, the acceleration of the chains is small so that we can ignore inertial effects. The separation D obeys an overdamped equation of motion, $\alpha dD/dt = 2F_x$, where F_x is the time-averaged force shown in Fig. 13 and α is an effective drag coefficient. Since we expect this approximation to be valid only for large separations, we have used the asymptotic form $F_x = 1300D^{-6}$ μN, where D is in millimeters. By solving the differential equation we can fit the predicted separation to the data and estimate the effective drag force on each chain. The calculated separation is shown as the line on Fig. 12, which is in very good agreement with the simulated motion for times greater than 5 s, where the velocity and acceleration are small. The corresponding value of α is 6×10^{-4} N m^{-1} s. If a chain in a semi-infinite fluid were to be approximated by a cylinder of the same length as the chain, α would be 1×10^{-4} N m^{-1} s [30]. The reasonable agreement between these numbers gives further support to the hypothesis that the repulsive force is due to streaming flows.

VII. COMMENTS ON PATTERN FORMATION

We have described in detail the evolution of the system from a collection of single particles to a configuration of stable chains. From Figs. 5 and 6 it appears that there is a well-defined separation of chains in the final state of the system. The simplest explanation for a periodic pattern would be the existence of a long-range attraction between chains and a short-range repulsion. However, in our simulations we were unable to identify an attraction between full chains.

An alternative explanation of the spacing between chains in our simulations comes from the fact that individual chain formation is a local ordering phenomenon: each chain is formed from particles in its immediate vicinity. If the initial distribution is on the average spatially homogeneous then the resulting chain structure will appear to be periodic, as in Fig. 6. On longer time scales, we have shown that two full chains repel each other weakly. However, for a large number of particles in a finite box, the full chains that form uniformly in the cell are unable to drift further apart because of the presence of the end walls. Consequently, the pattern will remain stable.

We have also carried out some simulations in which the spheres start clustered in the centre of the cell. Full chains rapidly form and subsequently spread out throughout the whole cell due to the weak repulsive interaction. The final configuration is close to that obtained starting from a fully dispersed distribution of spheres. In both cases, the spatial separation of chains is determined by the geometry of the cell.

It should be noted that frictional forces with the base of the cell have been neglected in our simulations. Provided the forces between chains are large compared to the frictional forces, this approximation can be justified. However, as the pattern evolves the forces between chains decrease and therefore, at longer time scales the frictional forces may eventually be large enough to stop the pattern evolving further. A detailed investigation of frictional effects for particles on a surface in an oscillating fluid is a challenging problem [9] and beyond the scope of this present study.

Chain formation has also been observed by Wunenburger *et al.* [9]. In their experiments, smaller particles were used in a much larger cell, with the particles always initially positioned as a clump in the center of the cell. Wunenburger *et al.* noted that the final separation of chains depended upon the vibratory conditions. By varying the vibratory conditions once a pattern had formed, the separation between chains could be made to increase or decrease. This observation suggested the existence of a long-range attraction between chains, although a mechanism for this attraction is still unknown. Our simulations have shown that particles are attracted to the free ends of chains due to the return streaming flows in the plane of the chains. In a large cell, provided the chains are far from the sidewalls, their free ends could attract neighboring chains, holding the pattern together. This may be an explanation for the attraction observed by Wunenburger *et al.* It would be interesting to investigate this possibility further.

ACKNOWLEDGMENTS

We are grateful to the Engineering and Physical Sciences Research Council for support, and to the workshop staff of the School of Physics and Astronomy for their skill and enthusiasm.

[1] I. S. Aranson and L. S. Tsimring, Rev. Mod. Phys. **78**, 641 (2006).
[2] F. Melo, P. B. Umbanhowar, and H. L. Swinney, Phys. Rev. Lett. **75**, 3838 (1995).
[3] T. Mullin, Phys. Rev. Lett. **84**, 4741 (2000).
[4] M. Faraday, Philos. Trans. R. Soc. London **121**, 299 (1831).
[5] P. Gondret and L. Petit, Phys. Fluids **8**, 2284 (1996).
[6] F. Zoueshtiagh and P. J. Thomas, Phys. Rev. E **61**, 5588 (2000).
[7] P. Sanchez, M. R. Swift, and P. J. King, Phys. Rev. Lett. **93**, 184302 (2004).
[8] D. Beysens, D. Chatain, P. Evesque, and Y. Garrabos, Europhys. Lett. **82**, 36003 (2008).
[9] R. Wunenburger, V. Carrier, and Y. Garrabos, Phys. Fluids **14**, 2350 (2002).
[10] N. Riley, Annu. Rev. Fluid Mech. **33**, 43 (2001).
[11] G. A. Voth, B. Bigger, M. R. Buckley, W. Losert, M. P. Brenner, H. A. Stone, and J. P. Gollub, Phys. Rev. Lett. **88**, 234301 (2002).
[12] D. Klotsa, M. R. Swift, R. M. Bowley, and P. J. King, Phys. Rev. E **76**, 056314 (2007).
[13] W. Kalthoff, S. Schwarzer, and H. J. Herrmann, Phys. Rev. E **56**, 2234 (1997).
[14] F. H. Harlow and J. E. Welch, Phys. Fluids **8**, 2182 (1965).
[15] K. Höfler and S. Schwarzer, Phys. Rev. E **61**, 7146 (2000).
[16] R. Peyret and T. D. Taylor, *Computational Methods for Fluid Flow*, Springer Series in Computational Physics (Springer, New York, 1983).
[17] M. P. Allen and D. J. Tildesley, *Computer Simulations of Liquids* (Clarendon Press, Oxford 1987).
[18] H. J. Herrmann and S. Luding, Continuum Mech. Thermodyn. **10**, 189 (1998).
[19] B. S. Massey, *Mechanics of Fluids* (Chapman and Hall, London 1968).
[20] N. Riley, Q. J. Mech. Appl. Math. **19**, 461 (1966).
[21] F. Otto, E. K. Riegler, and G. A. Voth, Phys. Fluids **20**, 093304 (2008).
[22] H. M. Blackburn, Phys. Fluids **14**, 3997 (2002).
[23] J. M. Andres and U. Ingard, J. Acoust. Soc. Am. **25**, 928 (1953).
[24] J. M. Andres and U. Ingard, J. Acoust. Soc. Am. **25**, 932 (1953).
[25] C. K. Kotas, M. Yoda, and P. H. Rogers, Exp. Fluids **42**, 111 (2007).
[26] S. Hassan, T. P. Lyubimova, D. V. Lyubimov, and M. Kawaji, Trans. ASME, J. Appl. Mech. **73**, 72 (2006).
[27] S. Hassan, T. P. Lyubimova, D. V. Lyubimov, and M. Kawaji, Int. J. Multiphase Flow **32**, 1037 (2006).
[28] D. V. Lyubimov, A. A. Cherepanov, T. P. Lyubimova, and B. Roux, J. Phys. IV **11**, 83 (2001).
[29] A. A. Ivanova, V. G. Kozlov, and A. F. Kuzaev, Dokl. Akad. Nauk **402**, 488 (2005) [Dokl. Phys. **50**, 311 (2005)].
[30] G. K. Batchelor, *An Introduction to Fluid Dynamics* (Cambridge University Press, Cambridge, U.K., 1967).